LIMNOLOGY and OCEANOGRAPHY LETTERS

ASLO

Open Access

Limnology and Oceanography Letters 10, 2025, 566–575

doi: 10.1002/lol2.70028

LETTER

Confirming existing parameterizations for methane gas transfer velocity in lakes based on direct and high-frequent methods

Leonie Esters,[1,2*] **Jan Kleint**,[3,4] **Torben Gentz**,[5] **Anna Rutgersson**,[1] **Marcus B. Wallin**,[6] **Hiroki Iwata**,[7] **Antonin Verlet-Banide**,[1] **Erik Sahlée**[1]

[1]Department of Earth Sciences, LUVAL, Uppsala University, Uppsala, Sweden; [2]Institute of Geosciences, University of Bonn, Bonn, Germany; [3]Organic Geochemistry, MARUM, University of Bremen, Bremen, Germany; [4]Institute of Earth Sciences, Heidelberg University, Heidelberg, Germany; [5]Marine Geochemistry, Alfred Wegener Institute, Bremerhaven, Germany; [6]Department of Aquatic Sciences and Assessment, Swedish University of Agricultural Sciences, Uppsala, Sweden; [7]Department of Environmental Science, Faculty of Science, Shinshu University, Matsumoto, Japan

Scientific Significance Statement

Methane is a greenhouse gas that has a greater warming potential than carbon dioxide. Lakes are known to release methane to the atmosphere. However, it is difficult to predict the exact amount of methane that is released from lakes. To reduce this uncertainty more measurements are needed. Until now, more measurements exist for carbon dioxide than there are for methane. In this study, we use a unique measurement setup in a freshwater lake in Sweden. The measurements from this setup show that methane from the lake is exchanged faster with the atmosphere when there are higher winds. Also, our results show that a similar amount of methane is released from the lake as would have been estimated using parameterizations based on carbon dioxide flux observations. Furthermore, faster methane exchange compared to CO_2 at wind speeds below 4 m s^{-1} can be explained by ebullition.

Abstract

Freshwater systems are important sources of atmospheric methane (CH_4). However, estimated emissions are associated with high uncertainties due to limited knowledge about the temporal variability in emissions and their associated controls, such as air–water gas transfer velocity. Here, we determined the gas transfer velocity of CH_4 based on a novel measurement setup that combines simultaneous eddy covariance flux measurements with continuously monitored CH_4 water- and air-side concentrations. Measurements were conducted during a 10-d campaign in a freshwater lake in mid-Sweden. The gas transfer velocity fell within the range of existing wind-speed-based parameterizations derived for carbon dioxide in other lakes. For wind speeds below 4 m s^{-1}, the gas transfer velocity for CH_4 followed parameterizations predicting faster gas exchange, while for wind speeds above 5 m s^{-1}, it aligned with those predicting relatively lower gas exchange. This pattern can be explained by ebullition. Extending the wind speed range for such combined eddy covariance measurements with continuously monitored CH_4 water- and air-side concentrations would improve model reliability.

*Correspondence: leonie.esters@geo.uu.se

Associate Editor: Alberto V. Borges

Data Availability Statement: Data and metadata are available at https://doi.org/10.57804/3xew-2472.

Freshwater systems (lakes, rivers and reservoirs) are the main global sources of methane (CH_4), but their spatiotemporal variability is poorly understood, leading to high uncertainty in emission estimates (IPCC 2021).

CH_4 is emitted from freshwaters via the main pathways diffusion, ebullition and plant-mediated transport from littoral vegetation (Bastviken 2009). The diffusive flux (F) depends on the concentration gradient between water and air and the gas transfer velocity (k):

$$F = k(C_w - C_{\mathrm{eq}}) \quad (1)$$

where C_w and C_{eq} are the CH_4 concentration in the surface water and air-equilibrium, respectively. k depends on many different processes like wind, waves, buoyancy, surfactants, etc. (Garbe et al. 2014).

To compare k for different gases and water temperatures, it can be normalized to a Schmidt number (Sc), of for example, 600, corresponding to CO_2 at 20°C in freshwater (Jähne et al. 1987). This assumes negligible effects from bubble-mediated gas exchange and gas solubility:

$$k_{600} = k(600/Sc)^n \quad (2)$$

where n is the Sc exponent, ranging from −2/3 to −1/2 based on lake surface conditions. Wave onset, influenced by wind speed, varies with lake conditions. Here, n is set to −1/2 assuming that surface waves, or some distortion of the surface, occurred throughout the study.

k is often parameterized using an empirical function based on wind speed derived from CO_2 flux observations. Previous studies have shown that k for CH_4 (k_{CH_4}) in lakes can differ from those for CO_2 (k_{CO_2}), both higher (Guérin et al. 2007; Prairie and del Giorgio 2013; Xaio et al. 2014; McGinnis et al. 2015; Paranaíba et al. 2018) and lower (Pajala et al. 2023). These differences indicate that the exchange of the two gases is partly controlled by different mechanisms. Microbubbles are, for example, suggested to explain higher k_{CH_4} relative to k_{CO_2} (Prairie and del Giorgio 2013; McGinnis et al. 2015; Paranaíba et al. 2018). We hypothesize that these differences manifest themselves in distinct wind speed dependencies, which we aim to investigate here.

The named studies that investigated differences in k between the two gases were based on floating chamber measurements, limited to local spot sampling with usually low time resolution. An alternative is the eddy covariance (EC) method (Aubinet et al. 2012), which offers advantages like representing a larger surface area in the upwind direction (footprint) and allowing continuous, high-frequency measurements. The spatial and temporal scales for estimating k vary significantly between methods (Klaus and Vachon 2020). Several studies have used the EC method for CO_2 on lakes (e.g., Podgrajsek et al. 2015; Esters et al. 2020; Golub et al. 2023; Jia et al. 2024), fewer for CH_4 (e.g., Podgrajsek et al. 2014a; Erkkilä et al. 2018; Iwata et al. 2018), and even fewer compare CO_2 with CH_4 (Sollberger et al. 2017).

Here, we conducted a 10-d field campaign at the Swedish lake Erken, performing continuous and simultaneous measurements of F_{CH_4} using EC along with CH_4 water- and air-side concentrations. This setup allowed us to continuously resolve k with the aim of evaluating how k_{CH_4} corresponds to current wind-speed based k_{CO_2} parameterizations. To our knowledge, this is the first direct determination of k from EC measurements for methane using continuous water- and air-side concentration measurements.

Methods

Lake Erken

Lake Erken (59°50.7233′N, 18°35.1716′E; Fig. 1) located in central Sweden, has a mean and maximum depth of 9 and 21 m, respectively, and a surface area of 24 km^2 (Pettersson et al. 2003). Atmospheric and water-side measurements were performed on and in connection to Malma island, a small and flat island located in the south-east of the lake (59°50.345′N, 18°37.774′E; Fig. 1). The areas of the lake facing the northern shore of the island are the deepest (∼ 15 m), while those facing the southern part of the island are shallower (∼ 5 m). During a field campaign from 19th to 29th of July 2017, the lake and atmospheric CH_4 concentration and EC F_{CH_4} were continuously measured (Esters et al. 2022).

Atmospheric measurements

Air–water F_{CH_4} were estimated using the EC method (e.g., Baldocchi and Meyers 1988; Aubinet et al. 2012). The measurements were taken from an 8-m tower, situated 0.5 m above the lake surface on Malma Island, with instruments 4.1 m above the tower base. A sonic anemometer (Wind Master, Gill Instruments) was used for measurements of the three wind components and temperature while an open path high precision and high-frequency methane analyzer (LI-7700, LI-COR) measured the atmospheric CH_4 concentration. High-frequency F_{CH_4} were determined from the raw 20-Hz EC measurements. The flux footprint was calculated following Kljun et al. (2015).

The tower was equipped with sensors for incoming solar radiation (CS300 Apogee), net radiation (CNR-4 Net Radiometer, Kipp & Zonen), air pressure (144SC0811, Sensortechnics GmbH), relative humidity (Rotronic AG), wind speed and direction (Wind Monitor, Young, at 2.5 and 6.2 m height). Wind speed at 6.2 m was recalculated to 10 m above the lake surface as u_{10} (see Supporting Information Section A1). Temperatures were measured at 1.9 and 6.0 m above the tower base (ventilated and radiation shielded thermocouples).

Prior to flux calculation, the high-frequency data was detrended and de-spiked, and a double rotation was applied to the sonic anemometer data. Then the flux was calculated for each 30-min period. Corrections (Webb et al. 1980) were applied to counteract density effects, with some modifications

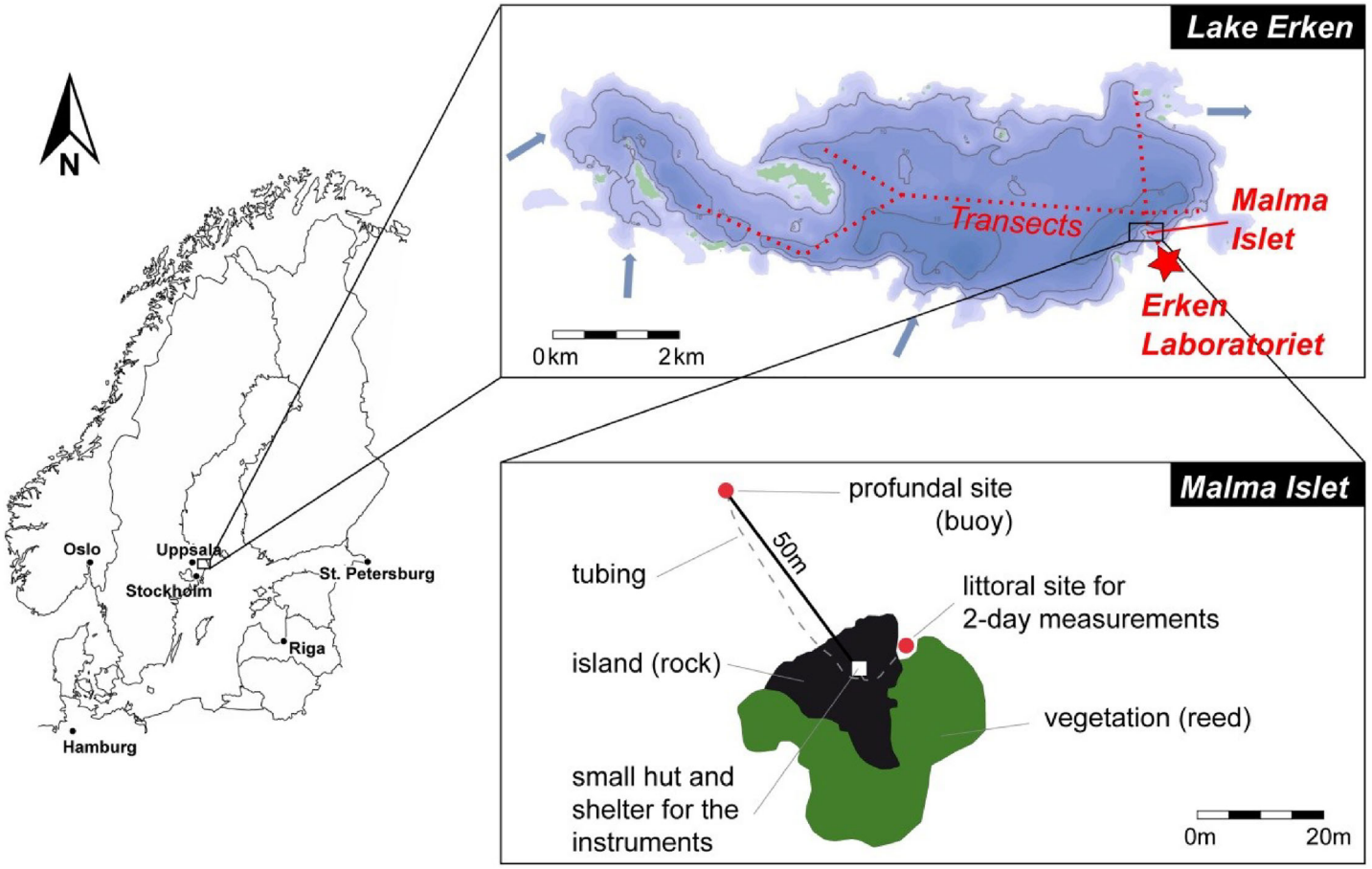

Fig. 1. Lake Erken, 100 km northeast of Stockholm, Sweden. Position of the sampling locations, transects (red dotted) and sampling sites for continuous measurements near Malma island at Lake Erken, sampled in July 2017. The bathymetric map of Lake Erken was modified after Eidborn (2015) and the arrows indicate stream inlets and outlets.

to the LI-7700 to compensate for the spectroscopic effects of temperature and atmospheric pressure (McDermitt et al. 2011).

Concentration values for which the received signal strength indication from the LI-7700 was lower than 10% were excluded from the analysis. This threshold has been used by Podgrajsek et al. (2014b) and Gutiérrez-Loza et al. (2019) (more details in Supporting Information Section A1).

Flux measurements influenced by land or disturbed by flow through the tower were excluded from the analysis (meaning wind directions between 40° and 200°). Following the quality control, 61 of the 30-min flux values remained, of which 4 were conducted at the shore site.

Water-side measurements

Water temperature was measured at 1-, 3-, and 15-m depth using an Aqua Oxygen Optode 4531 with a resolution of 0.01°C and an accuracy of ± 0.03°C. The water-side CH_4 concentrations ($[CH_4]_w$) were measured in the footprint of the tower by a new sampling system including a novel underwater membrane inlet mass spectrometer (UWMS) and a membrane-coupled portable cavity ring-down spectroscopy analyzer (Hartmann et al. 2018). Both instruments were operated from a hut at Malma island using a shared pumping system.

The UWMS was designed for underwater applications (Short et al. 2001; Bell et al. 2007; Schlüter and Gentz 2008) and redesigned to suit our applications (Gentz and Schlüter 2012). For the UWMS, water was pumped at a flow rate of 3 mL min^{-1} to the membrane inlet system. Gases permeating through the membrane were detected by an Inficon CPM 200 residual gas analyzer. During the membrane-coupled portable cavity ring-down spectroscopy deployment, the water flow was regulated to 500 ± 5 mL min^{-1}.

The membrane-coupled portable cavity ring-down spectroscopy was calibrated by a reference gas for CH_4 (5 ppm CH_4 and 500 ppm CO_2 in synthetic air) before, after, and every 8 h during measurements. The UWMS was calibrated twice a day by aquatic standards (contained 100 nmol L^{-1}, respectively, 1000 nmol L^{-1} CH_4) (Schlüter and Gentz 2008). The $[CH_4]_w$ data from the UWMS and membrane-coupled

portable cavity ring-down spectroscopy were validated by subsamples taken from the bypass during the deployment and measured in the laboratory thereafter. Due to maintenance and time-consuming calibration, both instruments suffered multiple downtimes. To achieve highest data density, the best performance of both instruments was combined, by merging their $[CH_4]_w$ data to a single data set (Fig. A1). By this, the $[CH_4]_w$ data showed an offset of less than 5% compared to the discrete samples.

From 19th to 22nd of July, lake water was pumped from the island shore from 1.0-m water depth. Thereafter, the submersible pump was deployed at a buoy in 2.5-m depth 50 m north of the island (Fig. 1). On the 27th, a profile of $[CH_4]_w$ (Fig. 3b) was performed next to the buoy (position in Fig. 1). On the 27th, discrete water samples were taken along two 7000- and 2300-m long transects at 0.5-m depth (Fig. 3a; Supporting Information Table A1) to detect spatial variations in $[CH_4]_w$.

Gas transfer velocity

The F_{CH_4} across the air–water interface is described using Fick's first law of diffusion (Eq. 1). Positive F_{CH_4} indicate fluxes from the water to the atmosphere. Following Eq. 1, measured F_{CH_4} allowed for calculating k_{CH_4} using the simultaneous measurements of surface water and atmospheric CH_4.

The air-equilibrium, eq.$[CH_4]_a$ was derived from the atmospheric partial pressure of CH_4 following Henry's law using the temperature dependent solubility (K_H), for CH_4 following Wiesenburg and Guinasso (1979):

$$\text{eq}[CH_4]_a = K_H \; pCH_{4_a} \tag{3}$$

with K_H in mol L^{-1} atm^{-1}.

Unfortunately, no simultaneous measurements of k_{CO_2} were made during the field campaign due to problems with the instruments measuring the water side concentration of CO_2.

Results

Environmental conditions

The environmental conditions during the experiment are summarized in Fig. 2. Most of the environmental variables followed a diurnal cycle. The atmospheric conditions were mainly unstable.

Methane concentration and flux

During the first 2 days of the campaign, $[CH_4]_w$ was measured at the littoral site (gray area in Fig. 2c–e), where the lake is shallower (1 m depth) compared to the buoy location (15 m depth). At the shallower site, $[CH_4]_w$ was higher with maximum values of up to 357 nmol L^{-1} (median: 253 nmol L^{-1}) compared to the deeper location with maximum values of 303 nmol L^{-1} (median: 240 nmol L^{-1}). Additionally, $[CH_4]_w$ was more variable at the shallower location than at the deeper location (interquartile range of 75 nmol L^{-1} compared to 39 nmol L^{-1}; Fig. 2e).

The eq.$[CH_4]_a$ was two orders of magnitude lower than $[CH_4]_w$ for the whole period (median of 3 nmol L^{-1} compared to 244 nmol L^{-1}) indicating a flux from the lake to the atmosphere. While eq.$[CH_4]_a$ showed higher values during nighttime than during daytime, it was in general less variable than $[CH_4]_w$ (interquartile range = 0.05 nmol L^{-1}). $[CH_4]_w$ was higher during lower wind speeds (median for u_{10} greater 5 m s^{-1} is 238 nmol L^{-1} relative to 248 nmol L^{-1} for u_{10} lower than 5 m s^{-1}). Thus, water–air CH_4 gradient increases at lower wind speeds as it mainly followed the variability of $[CH_4]_w$.

Measured F_{CH_4} ranged from 0.57 to 8.5 nmol m^{-2} s^{-1}, with a mean of 4.46 nmol m^{-2} s^{-1} and higher daytime values consistent with daily u_{10} variability.

The average footprint of the campaign of the EC measurements was 0.477 km long and 0.446 km wide (80% of the source area) with a peak footprint of 0.038 km long and 0.046 km wide (Supporting Information Fig. A1). The atmosphere was unstable for more than 90% of the time, thus the footprint size did not change much over the observation period. Within the footprint, $[CH_4]_w$ showed minimal spatial variation. Other areas, specifically near the shore, showed higher variability (Fig. 3a). $[CH_4]_w$ of the surface water at profundal sites ranged between 200 and 350 nmol L^{-1}, whereas the highest $[CH_4]_w$ (up to 1500 nmol L^{-1}) were found at littoral sites.

The $[CH_4]_w$ profile measured close to the buoy showed a mixed layer reaching down to 9 m (Fig. 3b) in which $[CH_4]_w$ varied between 220 and 260 nmol L^{-1}. $[CH_4]_w$ decreased to 117.5 nmol L^{-1} at 11 m depth and increased again closer to the bottom to 197.7 nmol L^{-1} at 14 m (lake depth is 15 m at this location).

Gas transfer velocity

k showed a temporal pattern similar to F_{CH_4}, ranging from 1.44 to 16.2 cm h^{-1}, with a mean of 9.84 cm h^{-1} (Fig. 2d). The highest k were observed during the 25th and 26th of July. Atmospheric conditions varied between the 2 days (Fig. 2a,b; Supporting Information Fig. A2): on the 25th, u_{10} exceeded 6.5 m s^{-1}, while on the 26th, it peaked at 5.1 m s^{-1}. F_{CH_4} on the 25th were lower (below 6.3 nmol m^{-2} s^{-1}) than on 26th (up to 9.7 nmol m^{-2} s^{-1}). The lower F_{CH_4} on 25 May coincided with a lower concentration gradient between water and air (median: 234 nmol L^{-1}), while the larger F_{CH_4} on 26 May were compensated by a higher concentration gradient (median: 273 nmol L^{-1}, driven by an increase in $[CH_4]_w$) to reach similar values of k.

Figure 4 shows the wind-speed dependence of k. A linear ($R^2 = 0.29$, root mean square error (RMSE) = 2.37 cm h^{-1}) and quadratic ($R^2 = 0.34$, RMSE = 2.45 cm h^{-1}) regression did not show much difference in explanatory power. For u_{10} between 2.0 and 3.2 m s^{-1} the observed k stayed below 9.2 cm h^{-1},

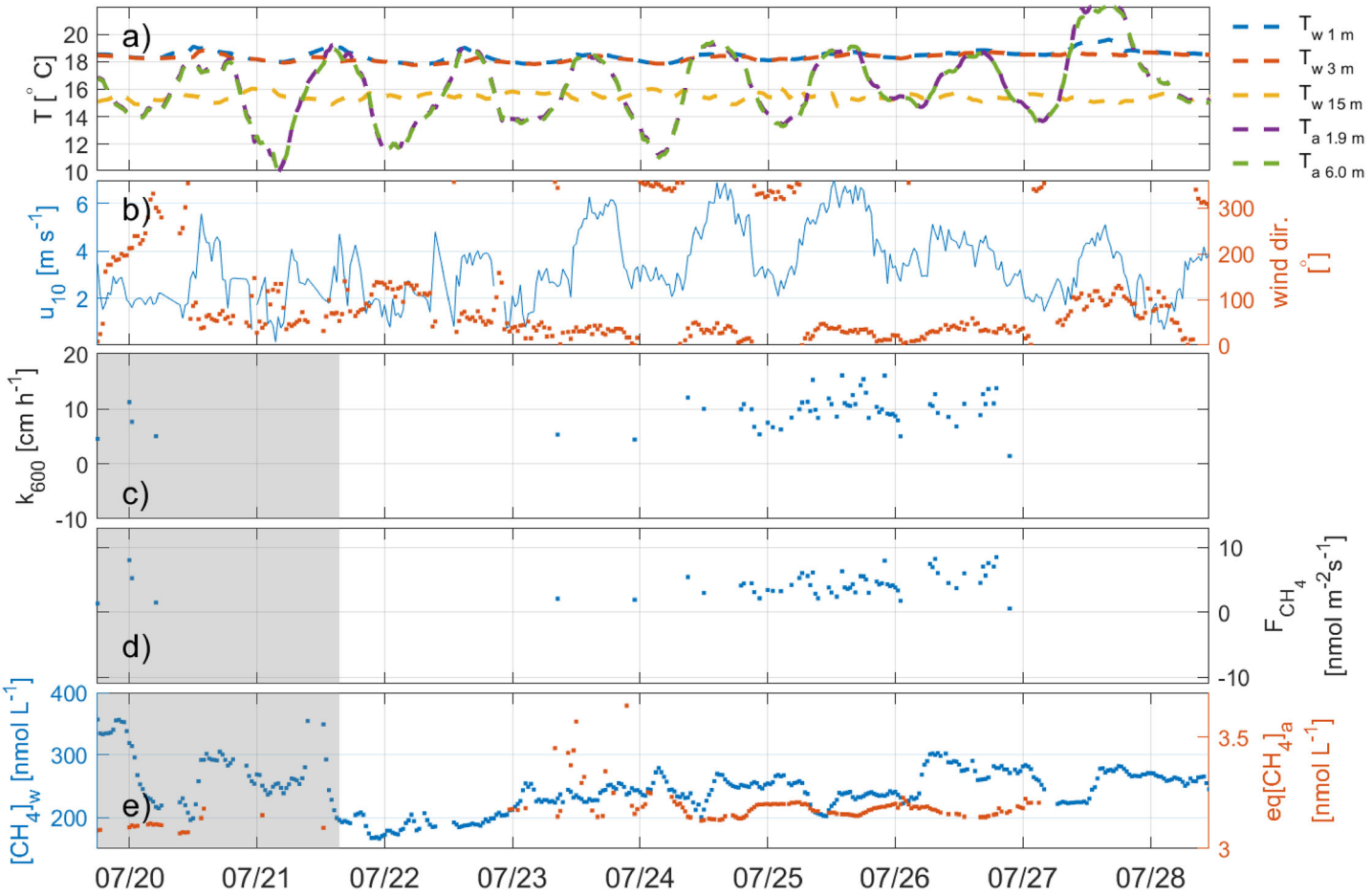

Fig. 2. Time series of (**a**) air temperature measured at two heights, $T_{a1.9m}$ at 1.9 m and $T_{a6.0m}$ at 6.0 m height, and water temperature measured at three depths, T_{w1m} at 1 m, T_{w3m} at 3 m, T_{w15m} at 15-m depth, (**b**) wind speed at 10 m (u_{10}) and wind direction, (**c**) gas transfer velocity (k) (**d**) CH_4 flux (F_{CH_4}), and (**e**) water and atmospheric CH_4 concentration, ([CH_4]$_w$ and eq.[CH_4]$_a$). The gray area shows the time in which the water concentration of CH_4 was sampled from a location close to the shore of Malma island.

while at u_{10} between 3.2 and 7.0 m s^{-1} they reached up to 16.1 cm h^{-1}. The enhanced k for u_{10} between 3.2 and 5.0 m s^{-1} reflected those measured during the 26th of July.

Discussion

Our measured k were in the range of k estimated by parameterizations derived from CO_2 measurements for other lakes (Jonsson et al. 2008; MacIntyre et al. 2010; Guérin et al. 2007; Sollberger et al. 2017; Vachon and Prairie 2013; Klaus and Vachon 2020). Although most of these parameterizations were derived from single lakes, the parameterizations by Klaus and Vachon 2020 represent a large-scale context from a global model and integrate data based on a range of tracer gases, including CO_2. The parameterization by Vachon and Prairie (2013) takes into account the lake area and the one by Klaus and Vachon (2020) additionally the footprint area.

In our measured wind speed range of 2.5 to 6.8 m s^{-1}, both a quadratic and linear regression match the CO_2 parameterizations (Fig. 4). For wind below 4 m s^{-1}, our bin averages align with parameterizations predicting faster gas exchange, as outlined by Vachon and Prairie (2013). Above 5 m s^{-1}, they align with parameterizations predicting lower exchange, similar to what was observed by Jonsson et al. (2008). Most of the parameterizations have negative Nash-Sutcliffe efficiency (NSE), indicating poor fit compared to the mean of the observed data (Sollberger et al. 2017: NSE = −0.10; Vachon et al. 2010: NSE = −0.12; Jonsson et al. 2008: NSE = −0.21; Guérin et al. 2007: NSE = −1.95). However, both models of Klaus and Vachon (2020) and MacIntyre et al. (2010) show a positive NSE (Klaus and Vachon 2020: NSE = 0.24 [linear] and NSE = 0.17 [power]; MacIntyre et al. 2010: NSE = 0.14), suggesting better but still improvable models.

Vachon and Prairie (2013) present CO_2 parameterizations for various lakes incorporating lake area logarithmically. Thus, small uncertainties in lake Erken's surface area would not significantly affect the estimated k. Their use of floating chambers can differ to EC method fluxes (Podgrajsek et al. 2014a).

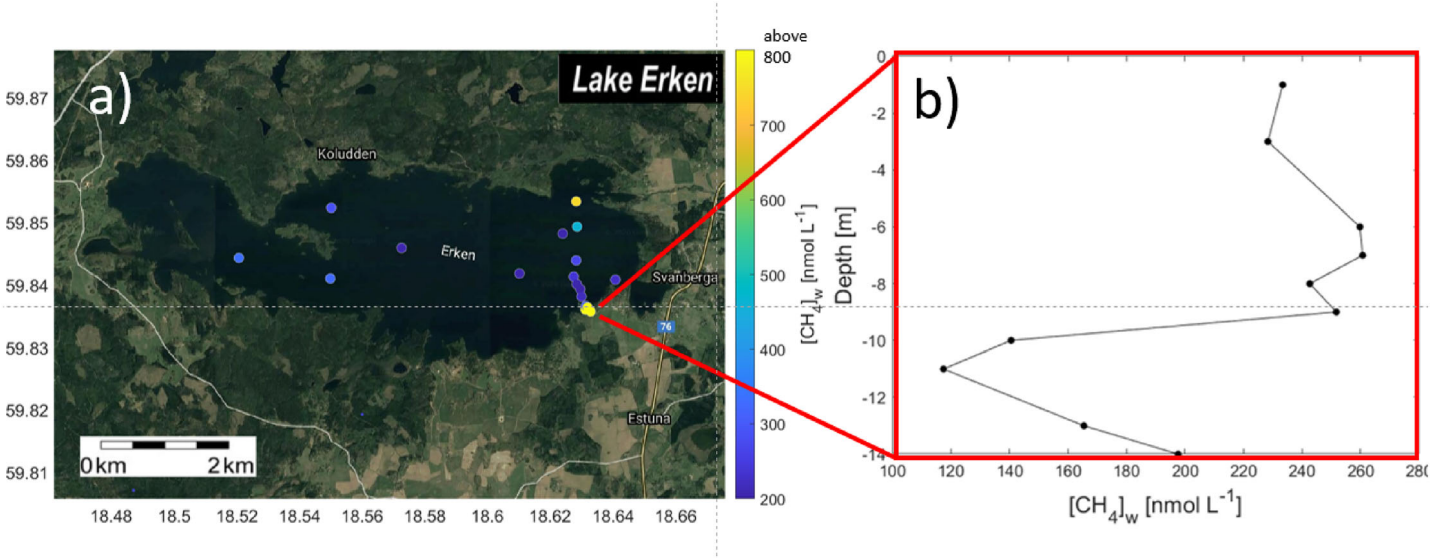

Fig. 3. (**a**) Map of Lake Erken with the location and concentration of the CH_4 water samples along transects (blue dots show lowest and yellow dots highest concentrations) and (**b**) a profile of the CH_4 concentration in the lake. The CH_4 profile was measured in the afternoon of the 27th of July and the transects were measured in the morning of the 28th of July.

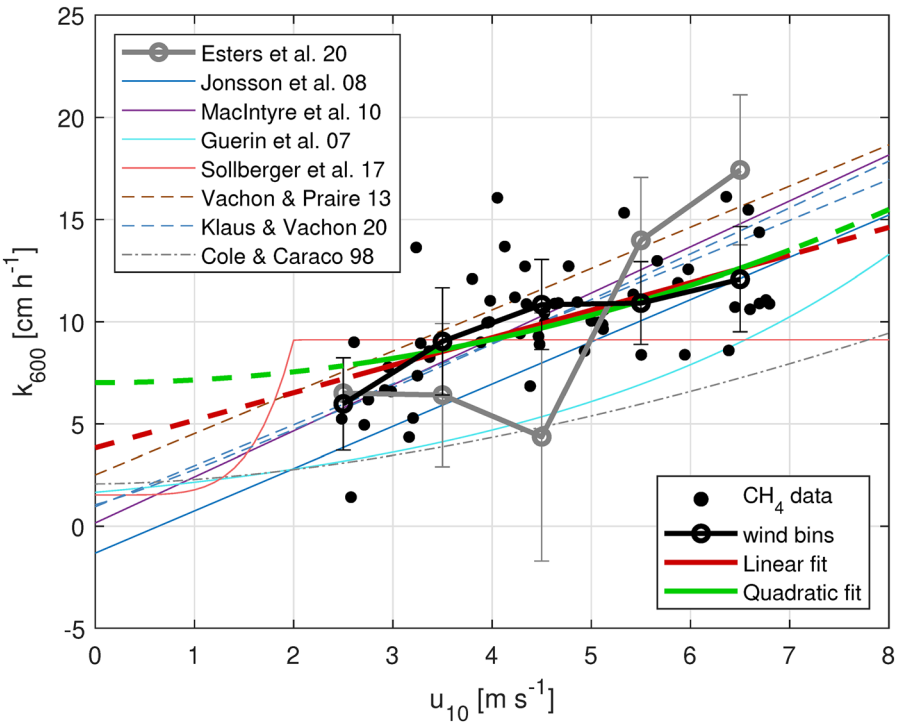

Fig. 4. Gas transfer velocity as a function of wind speed with the best fits through the data collected from our off-shore location represented by the bold green and red lines. As reference available parameterizations of k_{CO_2} from different methods, as well as bin-averaged k_{CO_2} from lake Erken for similar conditions of the presented 10-d field campaign are shown.

The model by Klaus and Vachon (2020) accounts for measurement type and best describes our data, showing our k_{CH_4} fits well in the global context of studies from different lakes, even when based on k_{CO_2}.

Since no simultaneous measurements of k_{CO_2} were conducted during the campaign, we compared our observations with measurements from the same site during 2014–2018 (Esters et al. 2020) in Fig. 4. We used k_{CO_2} data for periods

similar to our 10-d field campaign in terms of atmospheric stability, wind direction, buoyancy flux, footprint, and lake stratification, that is, July to August. This comparison shows that k_{CO_2} and k_{CH_4} at lake Erken are similar under similar stratified lake conditions, especially away from the shore. Thus, during such conditions, k_{CO_2} parameterizations can be applied to k_{CH_4}.

Our measured k_{CH_4} reaches up to 15 cm h^{-1} at winds near 4 m s^{-1}. MacIntyre et al. (2021) shows that diurnal heating results in k_{600} values from 8 to 16 cm h^{-1} at similar wind speeds. Their analyses are based on dissipation rates and meteorological data, independent of the gas being studied. This enhancement is not observed in k_{CO_2} from the 5-year period in Lake Erken, the median of which shows an increase toward lower $u_{10} < 4$ m s^{-1}. As we do not observe the described effects in k_{CO_2} but solely in k_{CH_4}, diurnal heating might play a secondary role in influencing the here observed gas transfer velocities.

Additional gas exchange mechanisms such as microbubbles or ebullition, could increase k for the sparingly soluble CH_4 relative to CO_2. Using the partitioning method by Iwata et al. (2018) on our EC flux measurements, we found that ebullition contributed most to the total flux at wind speeds below 5 m s^{-1} (Fig. 5). Higher bubble flux coincided with lower atmospheric pressure, facilitating CH_4 release from sediments. Here, it remains, however, uncertain if the observed changes in atmospheric pressure are sufficient to cause significant changes in hydrostatic pressure. This method, previously tested in systems where bubbling fluxes were 5–10 times higher than diffusive fluxes, may be less effective in our study with a lower ratio of bubble to diffusive flux. Microbubbles affect CH_4 more than CO_2 because of the lower solubility of CH_4, have been used to explain consistently higher k_{CH_4} than k_{CO_2} (Prairie and del Giorgio 2013; McGinnis et al. 2015).

Another important factor affecting k is the steadiness of wind speeds. Steady winds typically occurred near 6 or 2 m s^{-1}. Measurements at 4 m s^{-1} often represented changing wind speeds or directions. During decreasing winds, near-surface shear, which drives the turbulence moderating k values, can persist for some time, potentially increasing k, which might explain the observed higher k at 4 m s^{-1}. Additionally, rising winds from 2 to 4 m s^{-1} or 4 to 6 m s^{-1}, often coincided with warming water enhancing near-surface dissipation and thus increasing k values.

Our k_{CH_4} observations might be biased because $[CH_4]_w$ was measured at 2.5 m depth, potentially in a gradient in stratified lake conditions (Pajala et al. 2023) and might not fully capture the dynamics of the near-surface layer. This was the best achievable measurement and we lack a more detailed temperature profile to confirm the stratification.

Additional bias to the observed k_{CH_4} can be caused by non-local effects such as entrainment or advection. Esters et al. (2020) used a statistical method based on high-frequency data to identify the influence of erroneous fluxes from non-local sources to EC measurements. We applied the same technique, however could not detect any non-local influence, which depends on wind speed and fetch. The winds in our study were too low to cause any bias.

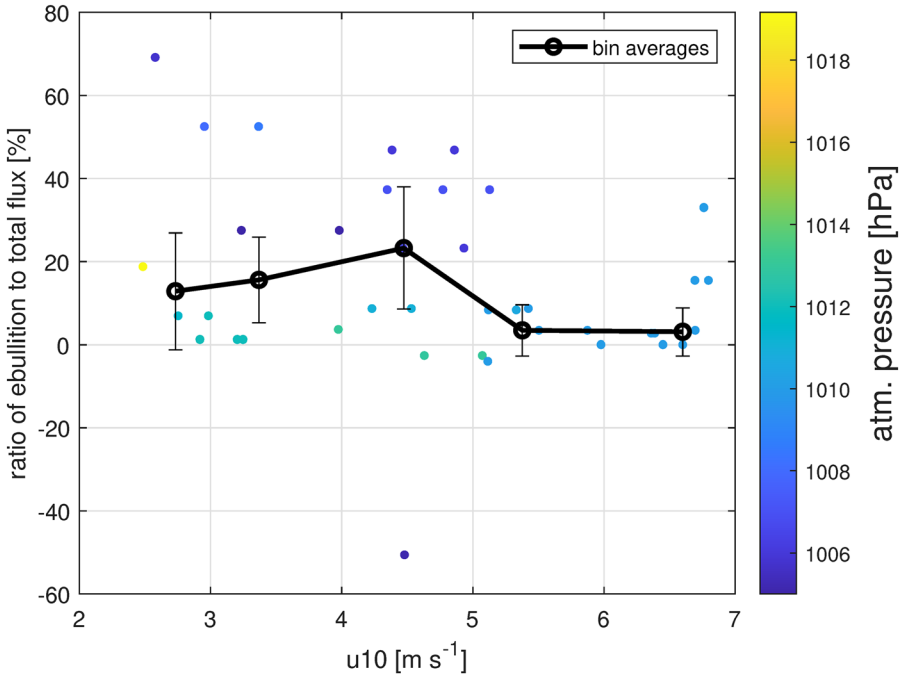

Fig. 5. Ratio of ebullition to total flux as a function of wind speed with the wind speed bin averages in red. The flux partitioning was performed following Iwata et al. (2018). The data is colored according to atmospheric pressure.

The $[CH_4]_w$ within the footprint area of the flux tower was homogeneous with low spatial variation (interquartile range = 42.5 nmol L^{-1}). Thus, a low influence on the measured k was expected due to the spatial variability of $[CH_4]_w$. However, extrapolations of k on the entire lake would need to consider the heterogeneity of $[CH_4]_w$.

Conclusion

We determined k_{CH_4} in lake Erken based on a unique combination of EC flux measurements and continuous atmospheric and water-side CH_4 concentration monitoring. Our results showed that k_{CH_4} is within the range of previously observed k_{CO_2} from lakes.

The measurements indicate that CH_4 exchanges more rapidly with the atmosphere under higher wind conditions. Furthermore, our results demonstrate that CH_4 flux estimates derived from CO_2-based parameterizations for other lakes accurately predict CH_4 emissions from Lake Erken. For wind speeds below 4 m s^{-1}, the measured k_{CH_4} aligns with parameterizations predicting faster gas exchange (Vachon et al. 2010), while for wind speeds above 5 m s^{-1}, they align with parameterizations predicting relatively lower exchange (Jonsson et al. 2008). This pattern can be explained by ebullition transport, which is highest during wind speeds below 5 m s^{-1} and is influenced by relatively low atmospheric pressure during these conditions.

More efforts are needed to verify and refine our results. This includes extending the wind speed range, meaning longer time series of combined EC flux measurements with continuous atmospheric and water-side CH_4 concentration. This would expand the range of environmental conditions such as the atmospheric pressure, crucial to accurately incorporate processes such as ebullition. Such efforts would improve the accuracy of CH_4 emission estimates from individual lakes to global scales.

Author Contributions

Erik Sahlée and Anna Rutgersson designed the study. Erik Sahlée, Antonin Verlet-Banide, Torben Gentz, and Jan Kleint performed the field measurements. Torben Gentz and Jan Kleint processed the aquatic CH_4 measurements. Erik Sahlée and Leonie Esters processed the atmospheric measurements. Hiroki Iwata performed the EC ebullition analysis. Leonie Esters performed the main data analysis with contributions by Anna Rutgersson, Marcus B. Wallin, Hiroki Iwata, and Erik Sahlée. Leonie Esters led the writing with contributions from all authors.

Acknowledgments

The staff at the Erken site are acknowledged for their great support during the experiment; many thanks to William Colom Montero, Don Pierson, Björn Mattsson, and Christer Strandberg. Lake Erken is part of SITES, Swedish Infrastructure for Ecosystem Science, funded by the Swedish Research Council under the grant number 2017-00635 and 2021-00164. The study was supported by funding from the Knut and Alice Wallenberg foundation (KAW 2013.0091).

Conflicts of Interest

There are no conflicts of Interest.

References

Aubinet, M., T. Vesala, and D. Papale. 2012. *Eddy Covariance: A Practical Guide to Measurement and Data Analysis*. Dordrecht: Springer.

Baldocchi, D. D., and T. P. Meyers. 1988. "Turbulence structure in a deciduous forest." *Boundary-Layer Meteorology* 43, no. 4: 345–364. https://doi.org/10.1007/BF00121712.

Bastviken, D. 2009. "Methane." In *Encyclopedia of Inland Waters*, edited by G. E. Likens, 783–805. Oxford: Academic Press. https://doi.org/10.1016/B978-012370626-3.00117-4.

Bell, R. J., R. T. Short, F. H. W. V. Amero, and R. H. Byrne. 2007. "Calibration of an In Situ Membrane Inlet Mass Spectrometer for Measurements of Dissolved Gases and Volatile Organics in Seawater." *Environmental Science & Technology* 41: 8123–8128. https://doi.org/10.1021/es070905d.

Eidborn, A. 2015. *Bathymetric Map of Lake Erken*. Sweden: Erken.

Erkkilä, K.-M., A. Ojala, D. Bastviken, et al. 2018. "Methane and Carbon Dioxide Fluxes over a Lake: Comparison between Eddy Covariance, Floating Chambers and Boundary Layer Method." *Biogeosciences* 15, no. 2: 429–445. https://doi.org/10.5194/bg-15-429-2018.

Esters, L., A. Rutgersson, E. Nilsson, and E. Sahlée. 2020. "Non-Local Impacts on Eddy-Covariance Air–Lake CO_2 Fluxes." *Boundary-Layer Meteorology* 178, no. 2: 283–300. https://doi.org/10.1007/s10546-020-00565-2.

Esters, L., A. Rutgersson, E. Sahlée, J. Kleint, T. Gentz, and A. Verlet-Banide. 2022. *Confirming Existing Parameterizations for Methane Gas Transfer Velocity in Lakes Based on Direct and High-Frequent Methods (Version 2)*. Sweden: Uppsala Universitet. https://doi.org/10.57804/3xew-2472.

Garbe, C. S., A. Rutgersson, J. Boutin, et al. 2014. "Transfer across the Air-Sea Interface." In *Ocean-Atmosphere Interactions of Gases and Particles*, edited by P. S. Liss and M. T. Johnson, 55–112. Berlin, Heidelberg: Springer Berlin Heidelberg. https://doi.org/10.1007/978-3-642-25643-1.

Gentz, T., and M. Schlüter. 2012. "Underwater Cryotrap-Membrane Inlet System (CTMIS) for Improved In Situ Analysis of Gases." *Limnology and Oceanography: Methods* 10: 317–328. https://doi.org/10.4319/lom.2012.10.317.

Golub, M., N. Koupaei-Abyazani, T. Vesala, et al. 2023. "Diel, Seasonal, and Inter-Annual Variation in Carbon Dioxide Effluxes from Lakes and Reservoirs." *Environmental Research*

Letters 18, no. 3: 034046. https://doi.org/10.1088/1748-9326/acb834.

Guérin, F., G. Abril, D. Serça, et al. 2007. "Gas Transfer Velocities of CO_2 and CH_4 in a Tropical Reservoir and its River Downstream." *Journal of Marine Systems* 66: 161–172. https://doi.org/10.1016/j.jmarsys.2006.03.019.

Gutiérrez-Loza, L., M. B. Wallin, E. Sahlée, et al. 2019. "Measurement of Air-Sea Methane Fluxes in the Baltic Sea Using the Eddy Covariance Method." *Frontiers in Earth Science* 7: 93. https://doi.org/10.3389/feart.2019.00093.

Hartmann, J. F., T. Gentz, A. Schiller, et al. 2018. "A Fast and Sensitive Method for the Continuous In Situ Determination of Dissolved Methane and Its δ13 C-Isotope Ratio in Surface Waters." *Limnology and Oceanography* 16, no. 5: 273–285. https://doi.org/10.1002/lom3.10244.

IPCC. 2021. *Climate Change 2021: The Physical Science Basis. Contribution of Working Group I to the Sixth Assessment Report of the Intergovernmental Panel on Climate Change*. Cambridge: Cambridge University Press.

Iwata, H., R. Hirata, Y. Takahashi, Y. Miyabara, M. Itoh, and K. Ilzuka. 2018. "Partitioning Eddy-Covariance Methane Fluxes from a Shallow Lake into Diffusive and Ebullitive Fluxes." *Boundary-Layer Meteorology* 169: 413–428. https://doi.org/10.1007/s10546-018-0383-1.

Jähne, B., G. Heinz, and W. Dietrich. 1987. "Measurement of the Diffusion Coefficients of Sparingly Soluble Gases in Water." *Journal of Geophysical Research* 92, no. C10: 10767–10776. https://doi.org/10.1029/JC092iC10p10767.

Jia, L., M. Zhang, W. Xiao, et al. 2024. "Aerosol Interference with Open-Path Eddy Covariance Measurement in a Lake Environment." *Agricultural and Forest Meteorology* 355: 110104. https://doi.org/10.1016/j.agrformet.2024.110104.

Jonsson, A., J. Aberg, A. Lindroth, and M. Jansson. 2008. "Gas Tranfer Rate and CO_2 Flux between an Unproductive Lake and the Atmosphere in Northern Sweden." *Journal of Geophysical Research* 113: G04006. https://doi.org/10.1029/2008JG000688.

Klaus, M., and D. Vachon. 2020. "Challenges of Predicting Gas Transfer Velocity from Wind Measurements over Global Lakes." *Aquatic Sciences* 82, no. 3: 53. https://doi.org/10.1007/s00027-020-00729-9.

Kljun, N., P. Calanca, M. W. Rotach, and H. P. Schmid. 2015. "A Simple Two-Dimensional Parameterisation for Flux Footprint Prediction (FFP)." *Geoscientific Model Development* 8: 3695–3713. https://doi.org/10.5194/gmd-8-3695-2015.

MacIntyre, S., D. Bastviken, L. Arneborg, et al. 2021. "Turbulence in a Small Boreal Lake: Consequences for Air–Water Gas Exchange." *Limnology and Oceanography* 66, no. 3: 827–854. https://doi.org/10.1002/lno.11645.

MacIntyre, S., A. Jonsson, M. Jansson, J. Aberg, D. E. Turney, and S. D. Miller. 2010. "Buoyancy Flux, Turbulence, and the Gas Transfer Coefficient in a Stratified Lake." *Geophysical Research Letters* 37, no. 24. https://doi.org/10.1029/2010GL044164.

McDermitt, D., G. Burba, L. Xu, et al. 2011. "A New Low-Power, Open-Path Instrument for Measuring Methane Flux by Eddy Covariance." *Applied Physics B: Lasers and Optics* 102: 391–405. https://doi.org/10.1007/s00340-010-4307-0.

McGinnis, D. F., G. Kirillin, K. W. Tang, et al. 2015. "Enhancing Surface Methane Fluxes from an Oligotrophic Lake: Exploring the Microbubble Hypothesis." *Environmental Science & Technology* 49, no. 2: 873–880. https://doi.org/10.1021/es503385d.

Pajala, G., D. Rudberg, M. Galfalk, et al. 2023. "Higher Apparent Gas Transfer Velocities for CO_2 Compared to CH_4 in Small Lakes." *Environmental Science & Technology* 57, no. 23: 8578–8587. https://doi.org/10.1021/acs.est.7b05138.

Paranaíba, J. R., N. Barros, R. Mendonça, et al. 2018. "Spatially Resolved Measurements of CO_2 and CH_4 Concentration and Gas-Exchange Velocity Highly Influence Carbon-Emission Estimates of Reservoirs." *Environmental Science & Technology* 52, no. 2: 607–615. https://doi.org/10.1021/acs.est.7b05138.

Pettersson, K., K. Grust, G. Weyhenmeyer, and T. Blenckner. 2003. "Seasonality of Chlorophyll and Nutrients in Lake Erken—Effects of Weather Conditions." *Hydrobiologia* 506: 1573–5117. https://doi.org/10.1023/B:HYDR.0000008582.61851.76.

Podgrajsek, E., E. Sahlée, D. Bastviken, et al. 2014*a*. "Comparison of Floating Chamber and Eddy Covariance Measurements of Lake Greenhouse Gas Fluxes." *Biogeosciences* 11, no. 15: 4225–4233. https://doi.org/10.5194/bg-11-4225-2014.

Podgrajsek, E., E. Sahlée, and A. Rutgersson. 2014*b*. "Diurnal Cycle of Lake Methane Flux." *Journal of Geophysical Research: Biogeosciences* 119: 236–248. https://doi.org/10.1002/2013JG002327.

Podgrajsek, E., E. Sahlée, and A. Rutgersson. 2015. "Diel Cycle of Lake-Air CO_2 Flux from a Shallow Lake and the Impact of Waterside Convection on the Transfer Velocity." *Journal of Geophysical Research. Biogeosciences* 120: 29–38. https://doi.org/10.1002/2014JG002781.

Prairie, Y. T., and P. A. del Giorgio. 2013. "A New Pathway of Freshwater Methane Emissions and the Putative Importance of Microbubbles." *Inland Waters* 3, no. 3: 311–320. https://doi.org/10.5268/IW-3.3.542.

Schlüter, M. P., and T. Gentz. 2008. "Application of Membrane Inlet Mass Spectrometry for Online and In Situ Analysis of Methane in Aquatic Environments." *Journal of the American Society for Mass Spectrometry* 19: 1395–1402. https://doi.org/10.1016/j.jasms.2008.07.021.

Short, R. T., D. P. Fries, M. L. Kerr, et al. 2001. "Underwater Mass Spectrometers for In Situ Chemical Analysis of the Hydrosphere." *Journal of the American Society for Mass Spectrometry* 12: 676–682. https://doi.org/10.1016/S1044-0305(01)00246-X.

Sollberger, S., B. Wehrli, C. J. Schubert, T. DelSontrol, and W. Eugster. 2017. "Minor methane emissions from an Alpine

hydropower reservoir based on monitoring of diel and seasonal variability." *Environ Sci Process Impacts* 19, no. 10: 1278–1291. https://doi.org/10.1039/c7em00232g.

Vachon, D., and Y. T. Prairie. 2013. "The Ecosystem Size and Shape Dependence of Gas Transfer Velocity Versus Wind Speed Relationships in Lakes." *Canadian Journal of Fisheries and Aquatic Sciences* 70, no. 12: 1757–1764. https://doi.org/10.1139/cjfas-2013-0241.

Vachon, D., Y. T. Prairie, and J. J. Cole. 2010. "The Relationship between Near–Surface Turbulence and Gas Transfer Velocity in Freshwater Systems and its Implications for Floating Chamber Measurements of Gas Exchange." *Limnology and Oceanography* 55, no. 4: 1723–1732. https://doi.org/10.4319/lo.2010.55.4.1723.

Webb, E. K., G. I. Pearman, and R. Leuning. 1980. "Correction of Flux Measurements for Density Effects Due to Heat and Water Vapour Transfer." *Quarterly Journal of the Royal Meteorological Society* 106: 85–100. https://doi.org/10.1002/qj.49710644707.

Wiesenburg, D. A., and N. L. Guinasso. 1979. "Equilibriumsolubilities of Methane, Carbon Monoxide, and Hydrogenin Water and Sea Water." *Journal of Chemical and Engineering Data* 24: 356–360. https://doi.org/10.1021/je60083a006.

Xaio, S., H. Yang, D. Liu, et al. 2014. "Gas Transfer Velocities of Methane and Carbon Dioxide in a Subtropical Shallow Pond." *Tellus B: Chemical and Physical Meteorology* 66, no. 1: 23795. https://doi.org/10.3402/tellusb.v66.23795.

Supporting Information

Additional Supporting Information may be found in the online version of this article.

Submitted 06 March 2024
Revised 03 May 2025
Accepted 06 May 2025